J. Applied Membrane Science & Technology, Vol. 29, No. 2, August 2025, 141–156
© Universiti Teknologi Malaysia

Underwater Oleophobicity of MBPP Membrane Modified by TiO_2/PDMS/IPA for Oil/Water Emulsion Separation

Marlisa Salamat, Chel-Ken Chiam* & Rosalam Sarbatly

Membrane and Nanomaterials Technology Research Laboratory,
Nanomaterials Research Centre, Faculty of Engineering, Universiti Malaysia Sabah,
Jalan UMS, 88400 Kota Kinabalu, Sabah, Malaysia

Submitted: 21/3/2025. Revised edition: 16/5/2025. Accepted: 16/5/2025. Available online: 1/8/2025

ABSTRACT

Meltblowing of polypropylene (PP) without using toxic solvents is a feasible method for mass-producing fibrous membranes for oil/water emulsion separation. However, the oleophilicity of PP can lead to fouling due to significant oil adsorption, and the low integrity of the PP fiber can cause the membrane structural failure during filtration operations. In this work, polydimethylsiloxane (PDMS) and isopropyl alcohol (IPA) are employed to improve the inter-fiber adhesion while maintaining the void structure that allows water permeation. Hydrophilic TiO_2 nanoparticles are deposited on the meltblown PP membrane (MBPP) using a suspension dispersion method, transforming the membrane into an underwater oleophobic surface. The results show that the TiO_2/PDMS/IPA modified MBPP membrane is oleophilic towards palm oil but oleophobic towards toluene under water. Because of the long chain and high molecular weight of triglycerides in palm oil, they form stronger intermolecular interactions with both the pristine and modified MBPP membrane surfaces. The underwater oil contact angle (UWOCA) of MBPP membrane varies between 5.1 ± 5° and 70.7 ± 6.3° when in contact with palm oil droplets. The UWOCA of toluene droplets increased from 67.4 ± 20.8° to 133.8 ± 18.1° when the TiO_2 loading was increased from 0 to 0.2 wt%. The optimal membrane with 0.2 wt% TiO_2 nanoparticles achieved the maximum flux at 25040 ± 2403 L/m^2 h and the separation efficiency > 99% for the toluene/water emulsion system. During the cyclic test, fouling from toluene adsorption occurred during cycle #3, but the separation efficiency remained greater than 98% after five cycles.

Keywords: Underwater oleophobic, meltblown polypropylene, membrane, TiO_2 nanoparticles, oil/water separation

1.0 INTRODUCTION

Oil spills are catastrophic environmental disasters that can have long-term effects on ecological diversity and the socioeconomic system. Wind and water currents cause oil pollution to spread [1, 2], increasing cleaning costs. Furthermore, this oily layer can prevent oxygen from entering the water, causing severe harm and even death for aquatic life [3]. Oil spills can pollute drinking water resources and endanger human health [4, 5].

Membrane filtration systems are well-known for having fewer mechanical parts, a simple flowsheet, a small footprint, no chemical additions, and easy startup and shutdown. Membrane filtration has been identified as a promising technique for oil/water separations [6–9]. Phase inversion is a well-established method for fabricating microstructure membranes for various applications

* Corresponding to: Chel-Ken Chiam (email: chiamchelken@ums.edu.my)
DOI: https://doi.org/10.11113/jamst.v29n2.314

[10, 11] such as oil-water separation [12, 13]. However, the microstructure formed in the membranes using the casting technique limits the membrane permeability, lengthens the separation processing time, and causes fouling. Fibrous structure membranes have recently received much attention in oil/water separation because of their higher water fluxes, oil rejections, and fouling resistances than phase inversion membranes [14, 15]. Electrospinning is a well-known and widely used method for creating fibrous membranes from homogeneous solutions. A sol is formed by dissolving a polymer in 80–90 wt% solvent. During the electrospinning process, a large volume of solvent is released into the air, which has become a major concern because the polymer solvents typically used are toxic and flammable, such as *N*-methyl-2-pyrrolidone, dimethylformamide, dimethylacetamide, and dimethyl sulfoxide [16, 17].

Meltblowing is a solvent-free extrusion technique that generates continuous nano/microfibers and forms a random web. Polymer granules are melted, then extruded through orifices blown by hot and high-velocity air into fine fibers, which are collected in the form of a mat on a suitable collector [18]. Meltblowing, unlike electrospinning, can produce fibrous membranes on a large scale because the polymer granules are not dissolved in any solvents during production. Nonetheless, the types of polymers that can be processed with meltblowing are limited. Polypropylene (PP) is the most viable polymer used to produce fibrous membranes using the meltblowing process [19]. The PP membrane has excellent chemical, acid, alkali, and solvent resistance [20]. Despite this, the PP membrane is oleophilic, meaning it is prone to organic adsorption, pore blockage, and requires frequent cleaning. To overcome this limitation, the PP membrane's oleophilicity must be transformed to oleophobicity in order to prevent pore blockage caused by organic adsorption while also exhibiting self-cleaning properties. Several techniques have been utilized to convert PP membranes into oleophobic ones, such as hydrolysis of 3-aminopropyltriethoxysilane (APTES) and self-polymerization of dopamine simultaneously in an alkaline aqueous solution [21], crosslinking with tannic acid, dopamine, and polyethyleneimine [22], construction of hierarchical micro/nano structures via the reaction of tea polyphenols and APTES [23], and titanium dioxide (TiO_2) coating by atomic layer deposition [24].

PP is a semi-rigid material with outstanding chemical and electrical properties. Nonetheless, during membrane formation, the PP fibers stack on top of one another, with poor inter-fiber adhesion. Severe structural fiber delamination, which causes fiber peeling from the membrane matrix, shortens membrane lifespan and limits cyclic use. However, the literature did not bridge this gap. This study attempted to improve the integrity of PP fibers by using polydimethylsiloxane (PDMS), a weak adhesive polymeric material. Strong adhesive polymers can tightly bind the fibers, reducing the volume of void between the fibers and thus reducing the water permeation flux. Araújo *et al*. [25] and Borók *et al*. [26] revealed PDMS to be a cost-effective binder for different composite substrates. However, PDMS has a low surface tension, which contributes to its hydrophobicity and resistance to water permeation. TiO_2 nanoparticle deposition can improve the hydrophilicity and water permeation flux of the membrane, as well as its oleophobicity, due to the abundance of

polar groups on the particle surface. Because the PP fiber and PDMS are anti-wetting, isopropyl alcohol (IPA) is used to hydrophilize the PDMS and combine it with the nanoparticles, resulting in a homogeneous mixture. On the other hand, most of the previous modified PP membrane studies tested the oil/water separation with relatively small molecules of hydrocarbon oils [21–23]. The influence of physical properties such as molecular weight and structure on the membrane surface wettability has received little attention in the literature. Therefore, the objective of this study is to determine the effect of TiO_2 nanoparticles on the underwater oleophobicity of a meltblown PP (MBPP) membrane modified with PDMS/IPA for toluene and palm oil, which have different molecular sizes and structures.

2.0 METHOD AND MATERIALS

2.1 Chemicals

Industrial-grade polypropylene (PP) powder was purchased from Sun-Allomer Ltd., Japan. Titanium dioxide (TiO_2), polydimethylsiloxane (PDMS), isopropyl alcohol (IPA) and hexane were purchased from Sigma-Aldrich. Buruh palm cooking oil was purchased at a local supermarket.

2.2 Fabrication of MBPP Membranes

PP fibers were produced using a Zetta Co. Ltd., Japan, meltblowing facility installed at Faculty of Engineering, Universiti Malaysia Sabah. PP powders were melted at 200-300°C, and the resulting PP molten was blown through a die with a 0.8-mm diameter hole using compressed air at 450°C. The MBPP membrane was collected from a distance of 240 cm from the die, as shown in Figure 1 (a). TiO_2 nanoparticles were dispersed in distilled water to form a suspension. Suspensions containing 0.2 to 0.4 wt% TiO_2 nanoparticles were prepared and homogenized for 5 minutes each. This range of nanoparticle loadings was widely used for fibers coating [27]. The suspension with a specific TiO_2 loading was then filtered through MBPP membranes at a vacuum pressure of 300 mmHg, as illustrated in Figure 1 (c). The membrane was dried at 60°C for 24 h before being immersed in a PDMS/IPA/distilled water mixture with a mass proportion of 5 g/10 g/85 g. The membranes were dried for three days at 60°C.

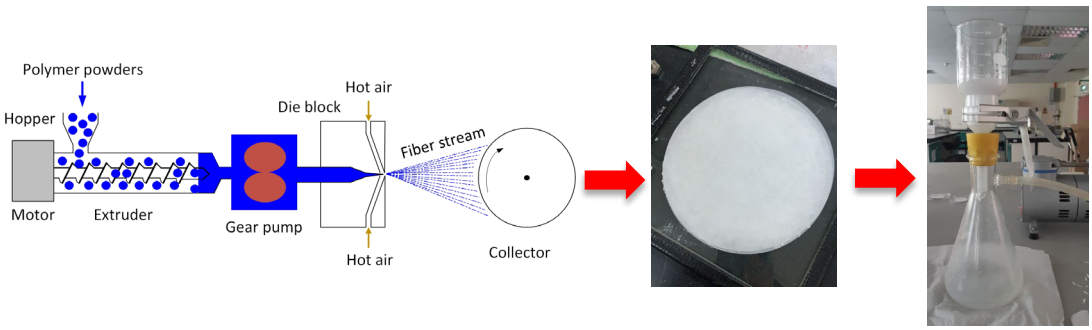

Figure 1 Fabrication and modification of MBPP membrane: (a) meltblowing of PP (b) pristine MBPP membrane, and (c) suspension dispersion of TiO_2 nanoparticles through vacuum filtration

2.3 Characterization of MBPP Membranes

2.3.1 Scanning Electron Microscopy (SEM) Analysis

A scanning electron microscopy (SEM, Hitachi S-3400) was used to observe the surface morphology of MBPP membranes at 15.0 kV with a scale of 500 μm. Prior to scanning, a thin gold layer was applied to each membrane sample.

2.3.2 Fourier Transform Infrared Spectroscopy (FTIR) Analysis

The chemical composition and functional groups of the MBPP membranes were analysed using a Fourier Transform Infrared Spectroscopy (FTIR, Perkin Elmer Frontier). The FTIR spectra were collected using the LabSolutions IR software, with a resolution of 4 cm^{-1} and a spectral range of 400 to 4000 cm^{-1}.

2.3.3 Contact Angle Analysis

A contact angle goniometer (Biolin Scientific) was used to assess the wetting properties of the surface modified MBPP membranes. Water contact angle was measured using the sessile drop method. A 6 μL droplet of water was dropped onto the membrane surface under atmospheric conditions. Following stabilisation, the water contact angles on both sides of the droplet were measured and averaged. The oil contact angle was measured underwater using the captive bubble method. The membrane sample was placed on the water surface in a beaker, and the modified surface of the membrane was positioned downward, making direct contact with the water. A 10 μL oil droplet was injected into the water, which rose up and touched the membrane surface. The oil contact angles on both sides of the droplet were measured and averaged as the droplet became more stable. The contact angles of each sample were measured at least three times at room temperature.

2.4 Separation Performance of MBPP Membranes

The oil/water separation was carried out using a dead-end filtration setup operating at 450 mmHg vacuum pressure. The oils that were tested were toluene and palm oil. The oil was mixed with water at a volume ratio of 1:99 and emulsified with 0.2 mg/mL Tween 80. The emulsions were vigorously stirred for 15 minutes. The emulsion was then routed to the dead-end filtration system, as illustrated in Figure 2. The flux and separation efficiency were determined using Equations (1) and (2), respectively [28].

$$J = \frac{V}{At} \tag{1}$$

where V is the volume of permeate, A is the effective membrane area, and t is the time of permeation.

$$SE = \frac{100\, m_p}{m_0} \tag{2}$$

where m_0 is the mass of water in feed, and m_p is the mass of water in permeate. An optimal membrane was then tested for reusability, with five cycles of filtration performed. Prior to the next filtration cycle, the reused membrane was rinsed with distilled water.

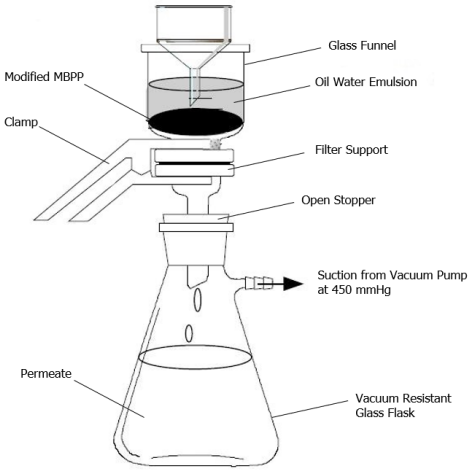

Figure 2 Dead-end filtration system for oil/water separation

3.0 RESULTS AND DISCUSSION

3.1 Morphology

The loading of TiO_2 nanoparticles has significantly altered the structure of the MBPP membrane surface, as shown in Figure 3.

Membranes with loadings of 0, 0.2, 0.3, and 0.4 wt% were identified as MBPP@T-0 (pristine), MBPP@T-0.2, MBPP@T-0.3, and MBPP@T-0.4, respectively. It is clear that as the nanoparticle content increases, the membrane surface area with fibrous structure decreases. The hydrophobic MBPP membrane tends to repel hydrophilic TiO_2 nanoparticles, preventing them from passing through during the vacuum filtration. As a result, as the nanoparticle loading increases, the surface coverage increases.

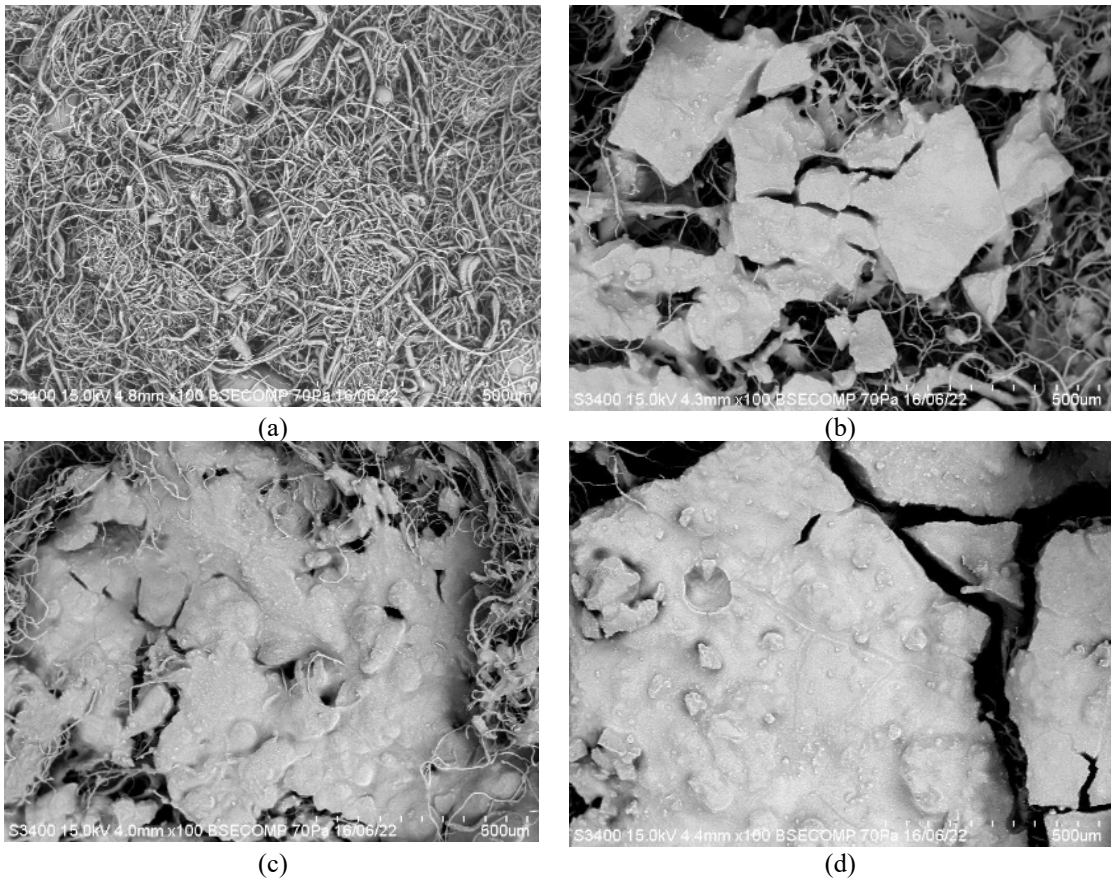

Figure 3 SEM images at 15.0 kV of potential with the scale at 500 μm for (a) pristine MBPP@T-0, (b) MBPP@T-0.2, (c) MBPP@T-0.3 and (d) MBPP@T-0.4 membranes with different loading of TiO2 at 0, 0.2, 0.3 and 0.4 wt%, respectively

3.2 Chemical Composition

The chemical compositions of pristine and modified MBPP membranes were investigated using FTIR, as illustrated in Figure 4. In the spectrum of pristine MBPP membrane, the spectra at 2928, 2916, 2874, and 2835 cm^{-1} describe the CH stretch [29]. Deformation vibrations of the plane methylene group have moderate absorption peaks in the spectral range of 1445–1485 cm^{-1}, while methyl group vibrations are designated in the range of 1430–1470 cm^{-1} or 1365–1395 cm^{-1} [30]. The peaks in our spectrum are at 1454 cm^{-1} and 1371 cm^{-1}, respectively. The transmittance peaks at 840, 1000, and 1170 cm^{-1} indicate the vibrations of terminal unsaturated CH_2 groups in isotatic PP [29,30]. The spectra in our work were obtained at 843, 970, and 1163 cm^{-1}. The transmittance peaks at 2964 and 2837 cm^{-1} indicate symmetric and asymmetric stretching vibrations of the $^{-}CH_3$ groups in Si–CH_3 of PDMS [31]. The spectra at 1454 cm^{-1} correspond to the vibration of CH_3 on PP, implying that the uncovered MBPP membrane surface. The peak at 1375 cm^{-1} can be attributed to the vibrations of carboxyl and methylene groups in TiO_2 [32]. Another band at 1259 and 1021 cm^{-1}, respectively, indicated symmetric CH_3 deformation and asymmetric Si–O–Si stretching [33]. The peaks 660 and 791 cm^{-1} in the range of 400–800 cm^{-1} are attributed to anatase.

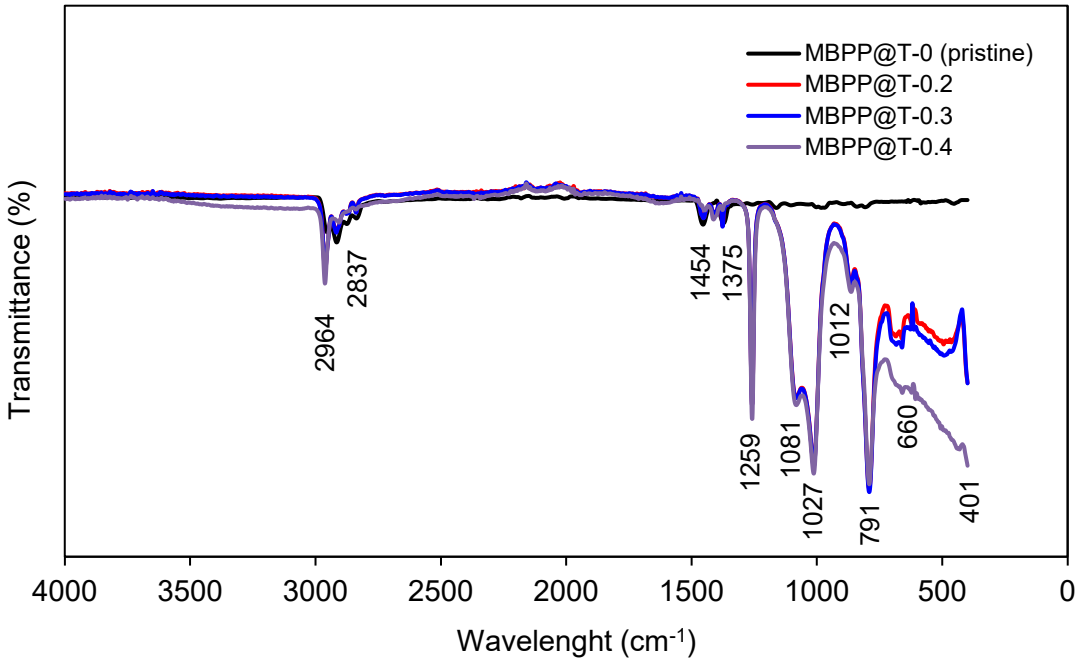

Figure 4 FTIR spectrum of the pristine and modified MBPP membranes

3.2 Surface Wettability

The chemical structure of PP is composed of strong C–H bonds and does not contain hydrophilic groups, so the pristine MBPP membrane is highly hydrophobic. Figure 5 (a) shows that the pristine MBPP membrane had a water contact angle (WCA) of 116.7°. The water droplet did not penetrate or diffuse through the membrane. TiO_2 nanoparticles have many reaction sites and hydroxyl groups that are easily hydrolyzed on their surface. Thus, the deposition of TiO_2 nanoparticles can modify the MBPP membrane to

become hydrophilic [34]. As shown in Figure 5 (b–d), the WCA decreased significantly, from approximately 77° to 67°, as the corresponding TiO_2 loading increased from 0.2 to 0.4 wt%, demonstrating the transformation of hydrophobicity to hydrophilicity. This observation is similar to that reported by Zou *et al*. [35]. When toluene and palm oil droplets came into contact with the surface of both pristine and modified MBPP membranes, they spread and penetrated immediately. These results confirm the superoleophilicity of both pristine and modified MBPP membranes. Furthermore, the modified MBPP membranes exhibit amphiphilicity in air, which is primarily due to the lyophilic IPA. The amphiphilicity of other modified membranes has also been reported in the literature [21, 36].

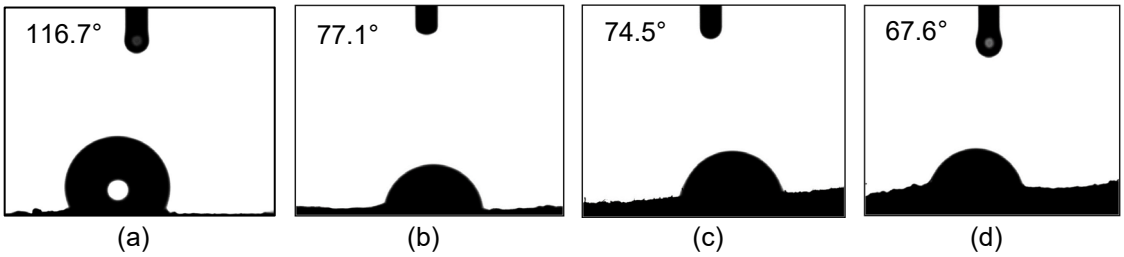

Figure 5 WCA of (a) pristine MBPP@T-0, (b) MBPP@T-0.2, (c) MBPP@T-0.3 and (d) MBPP@T-0.4 membranes

The instabilities of oil droplet formation and attachment on the membrane surface make the captive bubble measurement method of UWOCAs somewhat challenging, as shown in Figure 6. To reduce the measurement errors, at least 30 readings of UWOCAs taken at different times were considered for each membrane, and the average values of UWOCAs with their standard deviations were calculated, as shown in Figure 7. The pristine membrane has UWOCA values of 67.4 ± 20.8° for toluene and 5.1 ± 5° for palm oil droplets. This demonstrates that the pristine MBPP membrane is oleophilic under water. It's worth noting that palm oil had a higher affinity for the hydrophobic surface than toluene. Palm oil is made up of non-polar triglycerides with long chains, high molecular weight, and more viscous, which allows it to form stronger intermolecular interactions with the hydrophobic surface and enhanced adsorption [37]. In other words, oils with low viscosity and low molecular weight, such as toluene, have a lower affinity for the MBPP membrane surface than oils with high viscosity and molecular weight, such as palm oil. When the membrane was modified with TiO_2, the surface became oleophobic toward toluene while remaining oleophilic toward palm oil under water, despite increased UWOCAs. Compared to the PP membrane coated with TiO_2 using the atomic layer deposition method reported by Li *et al*. [24], the UWOCAs of the MBPP membranes coated by suspension deposition in this study were lower, i.e. less than 150°. This is because not all of the fibers' surfaces in the MBPP membranes were coated with TiO_2 nanoparticles, as evidenced by the SEM images shown in Figure 3. When the loading of TiO_2 nanoparticles was increased, the UWOCAs increased slightly at first and then decreased, possibly due to

TiO_2 nanoparticle agglomeration, which reduced the surface energy of the membranes [38,39]. As a result, the MBPP@T-0.2 membrane proved to be the optimal membrane in the current study.

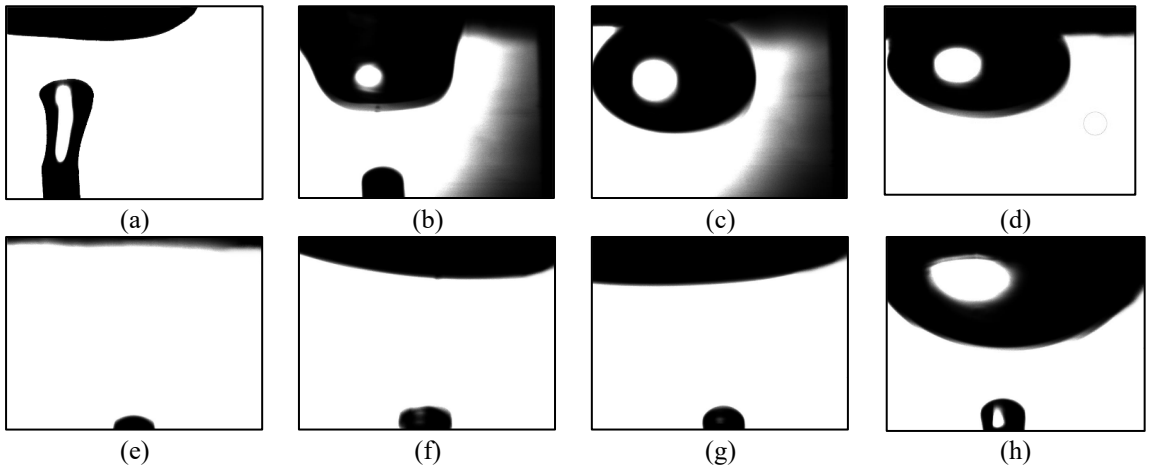

Figure 6 UWOCA of the (a, e) pristine MBPP@T-0, (b, f) MBPP@T-0.2, (c, g) MBPP@T-0.3 and (d, h) MBPP@T-0.4 membranes, for toluene droplets (a–d) and palm oil droplets (e–h)

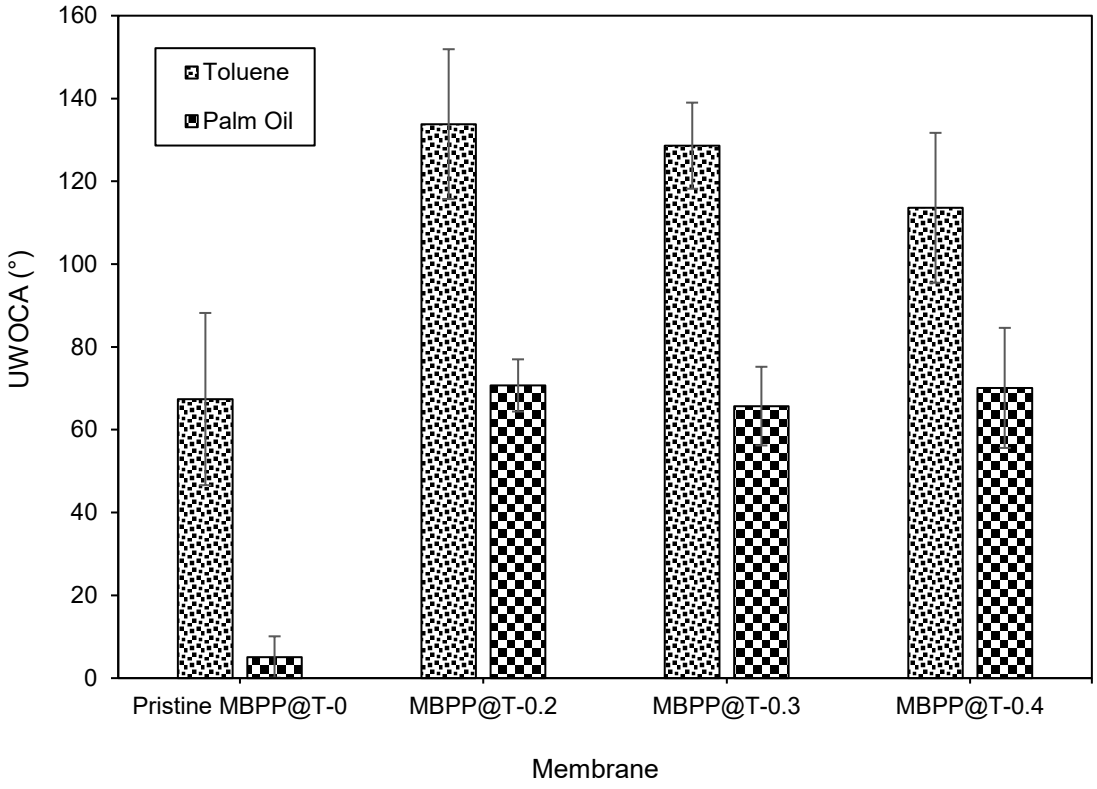

Figure 7 UWOCAs of toluene and palm oil droplets on pristine and modified MBPP membranes

3.3 Oil/water Separation and Reusability Experiments

Palm oil significantly adsorbs on MBPP membrane surfaces due to underwater oleophilicity (UWOCA < 90°) caused by large molecules and long chain triglycerides. As a result, permeation of the palm oil through the MBPP membranes occurred during the filtration, and milky permeates were observed as shown in Figure 8. (a). Similarly, Figure 8 (b) shows that toluene permeation was observed through the pristine MBPP membrane, which is also due to its underwater oleophilic properties. However, the toluene was successfully separated from water using the underwater oleophobic modified MBPP membranes, i.e., 90° < UWOCA < 150°. When the TiO_2 nanoparticle loading was increased from 0.2 to 0.4 wt%, the water permeation flux decreased significantly during the toluene/water emulsion separation process. The MBPP@T-0.2 membrane had the highest flux, while the MBPP@T-0.3 and MBPP@T-0.4 membranes had lower flux, possibly due to nanoparticle agglomeration, which resulted in a smaller pore size. This was also consistent with previous data from the current study and the literature [38,39]. Additionally, the membrane thickness increased when the TiO_2 nanoparticle loading increased, which escalated the water flow resistance [35]. A digital micrometer was used to measure membrane thickness. The pristine MBPP@T-0, MBPP@T-0.2, MBPP@T-0.3, and MBPP@T-0.4 membranes had thicknesses of 88.1, 90.6, 96.0, and 97.5 μm. Nevertheless, the separation efficiency of the toluene/water emulsion was more than 99%, as shown in Figure 9 (a).

The reusability of a membrane is critical for treating actual oily wastewater. In this study, the optimal membrane, MBPP@T-0.2, was tested for five cycles of toluene/water emulsion separation, as shown in Figure 9 (b). The flux and separation efficiency were measured during each cycle. Unlike the superhydrophilic modified PP membranes fabricated in the literatures [21,23], where the water droplets could rapidly permeate through the membranes within a few seconds, the water droplet stayed on the MBPP@T-0.2 membrane surface and was difficult to permeate, as shown in Figure 5 (b). As a result, a lower water permeation flux was observed, particularly during cycle #1, because water took longer time to fill and wet the newly formed membrane pores. When the wetted membrane from cycle #1 was reused, the water flux in cycle #2 increased significantly. However, the water fluxes began to decrease slightly from cycle #3, possibly due to the continuous adhesion and adsorption of toluene during the cyclic tests, which led to membrane fouling and difficult to be removed by simple water washing [22,23,40]. Despite this, the oil rejection was excellent throughout the cyclic tests, surpassing 98% of separation efficiency.

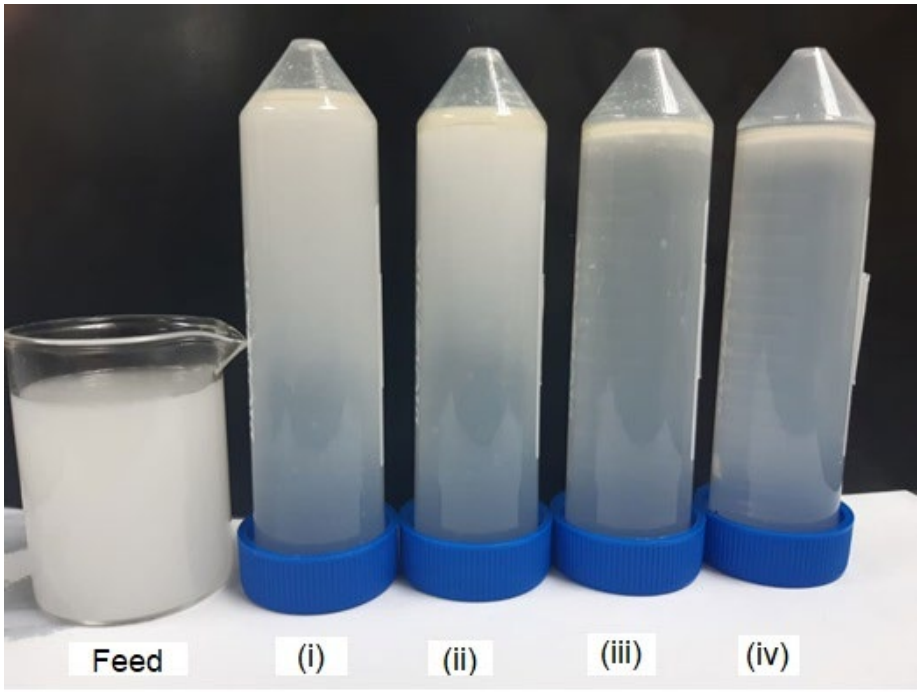

(a)

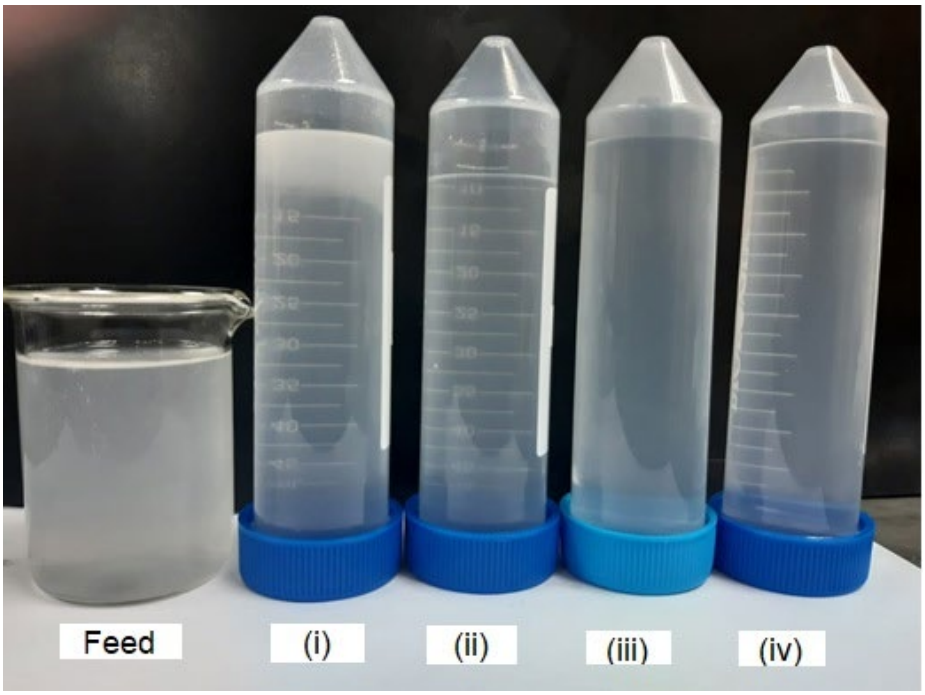

(b)

Figure 8 Separation of (a) palm oil/water emulsion and (b) toluene/water emulsion. Permeates collected by (i) pristine MBPP@T-0, (ii) MBPP@T-0.2, (iii) MBPP@T-0.3 and (iv) MBPP@T-0.4 membranes

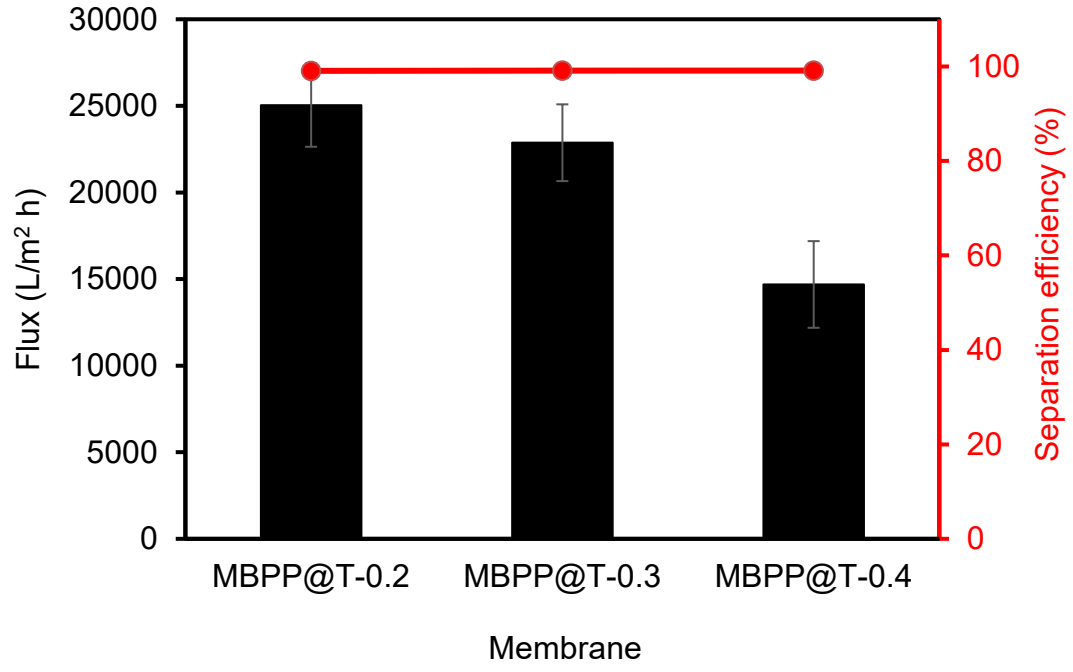

(a)

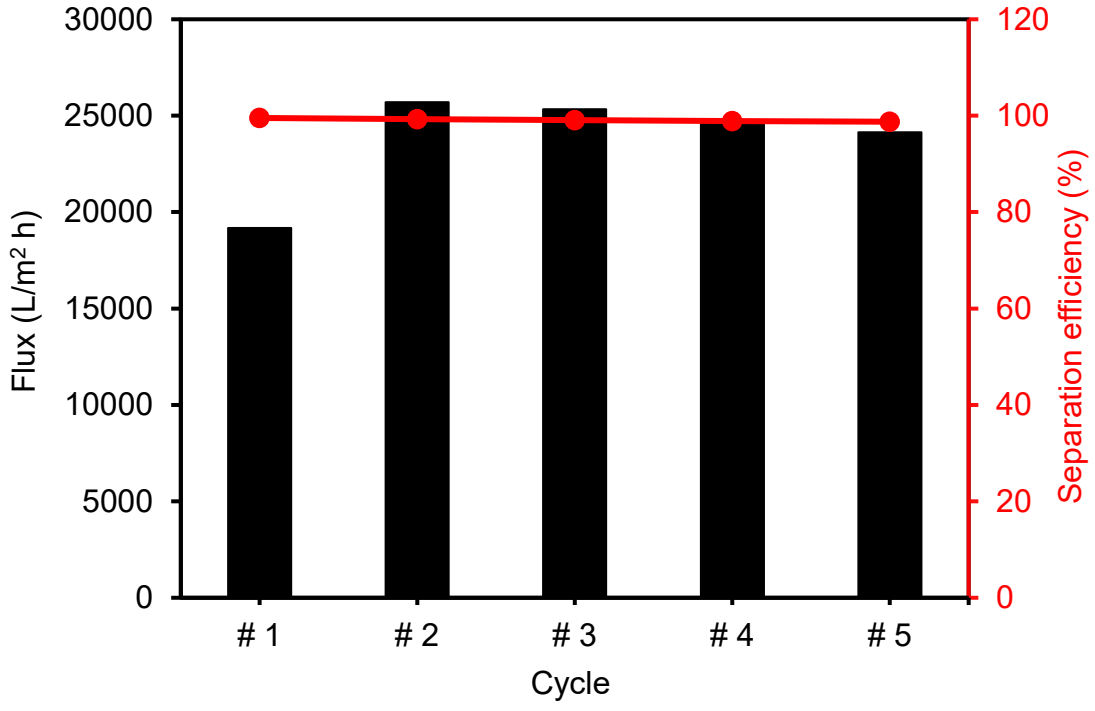

(b)

Figure 9 (a) The flux and separation efficiency of MBPP@T-0.2, MBPP@T-0.3 and MBPP@T-0.4 membranes for toluene/water emulsion. (b) The reusability of mbpp@T-0.2 Membrane for toluene/water emulsion separation

4.0 CONCLUSIONS

This study investigates TiO_2/PDMS/IPA modified MBPP membranes for the separation of toluene or palm oil from water. The wettability of the MBPP membrane can be altered by the deposition of TiO_2 nanoparticles via vacuum filtration. Because of the hydrophobic MBPP membrane's ability to retain hydrophilic TiO_2 nanoparticles, the nanoparticles cover the membrane surface, and the coverage increases as the nanoparticle load increases. As a result, the WCA of the MBPP membrane decreased from 116.7 to 67.6° as the nanoparticle loading increased from 0 to 0.4 wt%. Within this nanoparticle loading range, the MBPP membrane changed from hydrophobic to hydrophilic. The long chain and large molecular size of palm oil resulted in significant underwater oleophilicity, or adsorption rather than repellence, towards the modified MBPP membranes. Both pristine and modified MBPP membranes are superoleophilic toward toluene and palm oil. The modified MBPP membranes were amphiphilic in air. The MBPP@T-0.2 membrane achieved a maximum UWOCA of 133.8 ± 18.1°, a water permeation flux of 25040 ± 2403 L/m^2 h, and a separation efficiency of over 98% after five filtration cycles. Fouling caused by toluene adsorption occurred during cyclic filtration, and the simple water washing method is insufficient to completely remove the foulant.

ACKNOWLEDGEMENT

The authors wish to thank the research facilities provided by the Faculty of Engineering, Universiti Malaysia Sabah.

CONFLICTS OF INTEREST

The author(s) declare(s) that there is no conflict of interest regarding the publication of this paper.

REFERENCES

[1] Huettel, M. (2022). Oil pollution of beaches. *Current Opinion in Chemical Engineering, 36*, 100803. Doi: https://doi.org/10.1016/j.coche.2022.100803.

[2] Kuang, C., Chen, J., Wang, J., Qin, R., Fan, J., & Zou, Q. (2023). Effect of wind-wave-current interaction on oil spill in the Yangtze River estuary. *Journal of Marine Science and Engineering, 11*, 494. Doi: https://doi.org/10.3390/jmse11030494.

[3] Nukapothula, S., Wu, J., Chen, C., & Ali, Y. P. (2021). Potential impact of the extensive oil spill on primary productivity in the Red Sea waters. *Continental Shelf Research, 222*, 104437. Doi:https://doi.org/10.1016/j.csr.2021.104437.

[4] Ogunbiyi, O., Al-Rewaily, R., Saththasivam, J., Lawler, J., & Liu, Z. (2023). Oil spill management to prevent desalination plant shutdown from the perspectives of offshore cleanup, seawater intake and onshore pretreatment. *Desalination, 564*, 116780. Doi: https://doi.org/10.1016/j.desal.2023.116780.

[5] Sharma, K., Shah, G., Singhal, K., & Soni, V. (2024). Comprehensive insights into the impact of oil pollution on the environment. *Regional Studies in Marine Science, 74*, 103516. Doi:

https://doi.org/10.1016/j.rsma.2024.103516.

[6] Hussain, A., & Al-Yaari, M. (2021). Development of polymeric membranes for oil/water separation. *Membranes, 11*, 42. Doi: https://doi.org/10.3390/membranes11010042.

[7] Tai, M. H., Mohan, B. C., & Wang, C. H. (2022). Freeze-casting multicomponent aerogel membrane with controllable asymmetric multilayer configuration for high flux gravity-driven separation of oil-water emulsion. *Separation and Purification Technology, 293*, 121087. Doi: https://doi.org/10.1016/j.seppur.2022.121087.

[8] Li, Y., Fan, T., Cui, W., Wang, X., Ramakrishna, S., & Long, Y. (2023). Harsh environment-tolerant and robust PTFE@ZIF-8 fibrous membrane for efficient photocatalytic organic pollutants degradation and oil/water separation. *Separation and Purification Technology, 306*, 122586. Doi: https://doi.org/10.1016/j.seppur.2022.122586.

[9] Xu, M., Peng, W., Ruan, X., Chen, L., Dai, X., & Dai, J. (2023). Eco-friendly fabrication of porphyrin@hyperbranched polyamide-amine@phytic acid/PVDF membrane for superior oil-water separation and dye degradation. *Applied Surface Science, 608*, 155075. Doi: https://doi.org/10.1016/j.apsusc.2022.155075

[10] Zhou, J. Y., Luo, Z. Y., Yin, M. J., Wang, N., Qin, Z., Lee, K. R., & An, Q. F. (2020). A comprehensive study on phase inversion behaviour of a novel polysulfate membrane for high-performance ultrafiltration applications. *Journal of Membrane Science, 610*, 118404. Doi:https://doi.org/10.1016/j.memsci.2020.118404.

[11] Tang, Y., Lin, Y., Ma, W., & Wang, X. (2021). A review on microporous polyvinylidene fluoride membranes fabricated via thermally induced phase separation for MF/UF application. *Journal of Membrane Science, 639*, 119759. Doi:https://doi.org/10.1016/j.memsci.2021.119759.

[12] Bai, Z., Jia, K., Lin, G., Huang, Y., Liu, C., Liu, S., Zhang, S., & Liu, X. (2023). Solvent-nonsolvent regulated nano-functionalization of super-wetting membranes for sustainable oil/water separation. *Applied Surface Science, 613*, 156085. Doi: https://doi.org/10.1016/j.apsusc.2022.156085.

[13] Sadek, S. A., & Al-Jubouri, S. M. (2023). Structure and performance of polyvinylchloride microfiltration membranes improved by green silicon oxide nanoparticles for oil-in-water emulsion separation. *Materials Today Sustainability, 24*, 100600. Doi: https://doi.org/10.1016/j.mtsust.2023.100600.

[14] Sarbatly, R., & Chiam, C. K. (2022). An overview of recent progress in nanofiber membranes for oily wastewater treatment. *Nanomaterials, 12*, 2919. Doi: https://doi.org/10.3390/nano12172919.

[15] Diwan, T., Abudi, Z. N., Al-Furaiji, M. H., & Nijmeijer, A. (2023). A competitive study using electrospinning and phase inversion to prepare polymeric membranes for oil removal.

Membranes, 13, 474. Doi: https://doi.org/10.3390/membranes13050474.

[16] Naragund, V. S., & Panda, P. K. (2020). Electrospinning of cellulose acetate nanofiber membrane using methyl ethyl ketone and N, N-Dimethylacetamide as solvents. *Materials Chemistry and Physics, 240*, 122147. Doi: https://doi.org/10.1016/j.matchemphys.2019.122147.

[17] Askari, A., Nabavi, S. R., & Omrani, A. (2024). Fabrication of PES/PAN electrospun nanofiber membrane incorporated with [EMIM][Ac] ionic liquid for oil/water separation. *Journal of Water Process Engineering, 65*, 105768. Doi: https://doi.org/10.1016/j.jwpe.2024.105768

[18] Schmidt, J., Usgaonkar, S. S., Kumar, S., Lozano, K., & Ellison, C. J. (2022). Advances in melt blowing process simulations. *Industrial & Engineering Chemistry Research, 61*, 65–85. Doi: https://doi.org/10.1021/acs.iecr.1c03444.

[19] Hassan, M. A., Yeom, B. Y., Wilkie, A., Pourdeyhimi, B., & Khan, S. A. (2013). Fabrication of nanofiber membranes and their filtration properties. *Journal of Membrane Science, 427*, 336–344. Doi: https://doi.org/10.1016/j.memsci.2012.09.050.

[20] Ran, F. (2015). Polypropylene membrane. In E. Drioli & L. Giorno (Eds.), *Encyclopedia of membranes*. Springer. Doi: https://doi.org/10.1007/978-3-642-40872-4_1911-1.

[21] Sun, F., Li, T. T., Zhang, X., Shiu, B. C., Zhang, Y., Ren, H. T., Peng, H. K., Lin, J. H., & Lou, C. W. (2020). In situ growth polydopamine decorated polypropylene melt-blown membrane for highly efficient oil/water separation. *Chemosphere, 254*, 126873. Doi: https://doi.org/10.1016/j.chemosphere.2020.126873.

[22] Fang, S., Zhang, Z., Yang, H., Wang, G., Gu, L., Xia, L., Zeng, Z., & Zhu, L. (2020). Mussel-inspired hydrophilic modification of polypropylene membrane for oil-in-water emulsion separation. *Surface and Coatings Technology, 403*, 126375. Doi: https://doi.org/10.1016/j.surfcoat.2020.126375.

[23] Zhang, J., Wang, L., Zhang, H., Long, X., Zheng, Y., Zuo, Y., & Jiao, F. (2022). Biomimetic modified polypropylene membranes based on tea polyphenols for efficient oil/water separation. *Progress in Organic Coatings, 164*, 106723. Doi:https://doi.org/10.1016/j.porgcoat.2022.106723.

[24] Li, C., Ren, L., Zhang, C., Xu, W., & Liu, X. (2021). TiO_2 coated polypropylene membrane by atomic layer deposition for oil–water mixture separation. *Advanced Fiber Materials, 3*, 138–146. Doi: https://doi.org/10.1007/s42765-021-00069-9.

[25] Araújo, D. A. G., Pradela-Filho, L. A., Santos, A. L. R., Faria, A. M., Takeuchi, R. M., Karimi-Maleh, H., & Santos, A. L. (2019). Uncured polymethylsiloxane as binder agent for carbon paste electrodes: Application to the quantification of propranolol. *Journal of the Brazilian Chemical Society, 30*, 1988–1998. Doi:

https://doi.org/10.21577/0103-5053.20190117.

[26] Borók, A., Laboda, K., & Bonyár, A. (2021). PDMS bonding technologies for microfluidic applications: A review. *Biosensors, 11*, 292. Doi: https://doi.org/10.3390/bios11080292.

[27] Prasad, V., Sekar, K., Varghese, S., & Joseph, M. A. (2020). Evaluation of interlaminar fracture toughness and dynamic mechanical properties of nano TiO_2 coated flax fibre epoxy composites. *Polymer Testing, 91*, 106784. Doi: https://doi.org/10.1016/j.polymertesting.2020.106784.

[28] Yang, J., Cui, J., Xie, A., Dai, J., Li, C., & Yan, Y. (2021). Facile preparation of superhydrophilic/underwater superoleophobic cellulose membrane with $CaCO_3$ particles for oil/water separation. *Colloids and Surfaces A: Physicochemical and Engineering Aspects, 608*, 125583. Doi: https://doi.org/10.1016/j.colsurfa.2020.125583.

[29] Prabowo, I., Nur Pratama, J., & Chalid, M. (2017). The effect of modified ijuk fibers to crystallinity of polypropylene composite. *IOP Conference Series: Materials Science and Engineering, 223*, 012020. Doi: https://doi.org/10.1088/1757-899X/223/1/012020.

[30] Krylova, V., & Dukštienė, N. (2013). Synthesis and characterization of Ag_2S layers formed on polypropylene. *Journal of Chemistry, 2013*, 987879. Doi: https://doi.org/10.1155/2013/987879.

[31] Hamouni, S., Arous, O., Abdessemed, D., Nezzal, G., & Bruggen, V. (2019). Alcohol and alkane organic extraction using pervaporation process. *Macromolecular Symposia, 386*, 1800247. Doi: https://doi.org/10.1002/masy.201800247.

[32] Praveen, P., Viruthagiri, G., Mugundan, S., & Shanmugam, N. (2014). Structural, optical and morphological analyses of pristine titanium dioxide nanoparticles – Synthesized via sol–gel route. *Spectrochimica Acta Part A: Molecular and Biomolecular Spectroscopy, 117*, 622–629. Doi: https://doi.org/10.1016/j.saa.2013.09.037.

[33] Atta, A., & Abdeltwab, E. (2022). Influence of ion irradiation on the surface properties of silver-coated flexible PDMS polymeric films. *Brazilian Journal of Physics, 52*, 3. Doi: https://doi.org/10.1007/s13538-021-01011-5.

[34] Du, C., Wang, Z., Liu, G., Wang, W., & Yu, D. (2021). One-step electrospinning PVDF/PVP–TiO_2 hydrophilic nanofiber membrane with strong oil–water separation and anti-fouling property. *Colloids and Surfaces A: Physicochemical and Engineering Aspects, 624*, 126790. Doi: https://doi.org/10.1016/j.colsurfa.2021.126790.

[35] Zou, D., Kim, H. W., Jeon, S. M., & Lee, Y. M. (2022). Robust PVDF/PSF hollow-fiber membranes modified with inorganic TiO_2 particles for enhanced oil–water separation. *Journal of Membrane Science, 652*, 120470. Doi: https://doi.org/10.1016/j.memsci.2022.120470.

[36] Bao, Z., Chen, D., Li, N., Xu, Q., Li, H., He, J., & Lu, J. (2020). Superamphiphilic and underwater superoleophobic membrane for oil/water emulsion separation and organic dye degradation. *Journal of Membrane Science, 590*, 117804. Doi:https://doi.org/10.1016/j.memsci.2019.117804.

[37] Li, J., Wang, Q., Tao, J., Yan, B., & Chen, G. (2020). Experimental and comprehensive evaluation of vegetable oils for biomass tar absorption. *ACS Omega, 5*, 19579–19588. Doi: https://doi.org/10.1021/acsomega.0c02050.

[38] Pan, Z., Cao, S., Li, J., Du, Z., & Cheng, F. (2019). Anti-fouling TiO_2 nanowires membrane for oil/water separation: Synergetic effects of wettability and pore size. *Journal of Membrane Science, 572*, 596–606. Doi: https://doi.org/10.1016/j.memsci.2018.11.056.

[39] Han, L., Shen, L., Lin, H., Huang, Z., Xu, Y., Li, R., Li, B., Chen, C., Yu, W., & Teng, J. (2023). 3D printing titanium dioxide–acrylonitrile–butadiene–styrene (TiO_2–ABS) composite membrane for efficient oil/water separation. *Chemosphere, 315*, 137791. Doi: https://doi.org/10.1016/j.chemosphere.2023.137791.

[40] Zeng, Q., Zhao, D. L., Shen, L., Lin, H., Kong, N., Han, L., Chen, C., Teng, J., Tang, C., & Chun, T. S. (2023). Titanium oxide nanotubes intercalated two-dimensional MXene composite membrane with exceptional antifouling and self-cleaning properties for oil/water separation. *Chemical Engineering Journal, 474*, 145579. Doi: https://doi.org/10.1016/j.cej.2023.145579.